

# Walking Goal Line Detection Based on DM6437 on Harvesting Robot

Gang Wu, Yu Tan\*, Yongjun Zheng, and Shumao Wang

College of Engineering, China Agricultural University, Beijing, China  
wugang19771121@163.com, tanyu32@sina.com,  
{zyj,wangshumao}@cau.edu.cn

**Abstract.** As to aided driving by harvesting robot, there is the large amount of image data processing, meanwhile, harvesting robot requires real-time image processing and to calculate the linear parameters in a straight line detection of the walking target process. This paper presents a hardware processing platform to TMS320DM6437 digital signal processor as the core processing chip, and an improved Hough transform algorithm which is based on a determined point is proposed to complete line detection. A camera is to be fitted on the left top of the combine harvester in order to capture images of farmland scenes in the process of harvesting. At first, according to different color characteristics of harvested areas and non-harvested areas, improved methods of Maximum entropy threshold segmentation and morphological approach are employed to determine candidate points of walking goal line. Then the candidate points are selected as the point set. Finally, the improved Hough transform based on a determined point is applied to complete line detection. The algorithm simplifies binary map to unitary map. Comparing with the traditional Hough transform, it saves computing time, and reduces the parameter space greatly. After multiple images processing, tests show that this detection method can detect real-time parameters of harvesting robot's walking goal line, and the algorithm is well proved with respect to its speed, anti-interference and accuracy.

**Keywords:** TMS320DM6437, Harvesting Robot, Line Detection, Hough Transform.

## 1 Introduction

Autonomous navigation research of Agricultural robot is the requirements of modern agricultural development, and it also has become a high-tech research direction such as intelligent control in the application of agricultural machinery and equipment. Currently, the ways of agricultural robot navigation are as follows: (1) Beacon navigation. Namely, beacons are set on the determined points of work environment; (2) Global Positioning

---

\* Corresponding author.

System (GPS). The emergence of GPS is a major breakthrough of modern navigation technology, and it has high accuracy, unlimited users, all-weather work and other advantages. But it has a poor anti-interference ability. When it is obstructed by trees, houses and other blocks, the signal may be occasional lost; (3) Visual navigation. Visual navigation of agricultural autonomous walking robot, usually divides into two kinds: wireless guide and wired guide. Because of the complex operating environment of agriculture, we usually use wireless navigation, which robots accord a CCD camera's real-time detection of the surrounding environment to plan the required path, and it can follow the path without human intervention to move towards the target. Among them, due to its application is flexible and easy, visual navigation has become popular navigation way [1~3]. Agricultural robot's visual navigation requires not only an effective image processing algorithm, but also requires a stable platform of image processing with high executing speed and miniaturization. With the development of electronic technology, the signal processing hardware platform based on DSP [4~5] has been applied in image processing widely. This paper applies DSP hardware platform to complete image acquisition, image processing, external communications and other functions, at the same time, this hardware is very small, which applies improved Hough transform algorithm based on a determined point in the software.

## 2 System Hardware Components

System hardware consists of the signal processor TMS320DM6437, DSP program memory FLASH, and high-speed video A/D acquisition chip tvp5416. System hardware schematic diagram is shown in Fig.1. Firstly, TMS320DM6437 controls tvp5416 to do A/D conversion of the input analog video through the I2C bus and gets the digitized video signal. Then, image processing algorithms is used to detect linear parameters. Finally, the linear parameters by serial communication are sent to the steering control unit and the image is transmitted to the display unit.

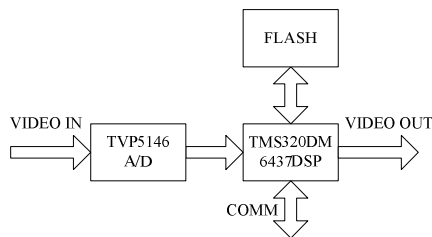


**Fig. 1.** System hardware schematic diagram

### 2.1 A/D Converter

Among the AD converter, there is a professional video A/D chip tvp5146 [6]. The chips do not need to use others to separate horizontal and vertical sync signals of video signal,

because it can get vertical sync signals from the composite video signal. By horizontal and vertical sync signals, it can collect A/D converted digital images correctly. The chip programs the input original image via I2C bus and controls image brightness, contrasts and outputs effective range. In practice, the original composite video signal of camera outputting is selected to do pretreatment according to field in the A/D chip, and then the resulting digital video signal is put into the DSP.

## 2.2 High-Speed Image Processing Unit

TMS320DM6437 from TI company is introduced in 2006, specifically for high-performance, low-cost video application development, frequency of 600MHz and 32-bit fixed point DSP Leonardo (DaVinci (TM)) technology processor family, it can be applied to automotive vision, robotics and other fields [7]. TMS320DM6437 uses the TMS320C64x+DSP as its core which is TI's third-generation-long instruction set architecture (VelociTI.3), clocks at up to 600MHz, supporting eight 8-bit or four 16-bit parallel MAC operations, and the peak capacity up to 4800MIPS. It can also handle H.264 encoding algorithm of 8 channels CIF or 3 channels D1 format. DM6437 provides video-on-chip input/output interfaces which are called video subsystem VPSS. DM6437 video subsystem is composed by two parts, and one is video processing front end for digital video input data, which provides the input interface for a variety of standard digital video, at the same time, it also makes necessary pre-processing for the input digital video data. The other is the video processing back end, and it is used to output digital video data to drive the display video images.

Therefore, here we use DM6437, external 27M crystal, by frequency to 600MHz. The program is written into FLASH, and then the program is loaded into the DSP by the power.

## 3 Line Detection Algorithm

The imaging system is designed to detect the navigation path line when harvest wheat by combine-harvester. As the combine harvester unloading grain port is on the left, so we usually choose the left part to start harvesting, and it is easy to unload the grain, even the right direction of driving is non-harvested area, and the left is harvested area. The most common route methods of harvesting are dextrorotation method and four sides harvest method [8], and dextrorotation method is suitable for longer but not wider farmland. After cutting out of road, the long side direction of the harvest is followed, then the combine-harvester needn't to head back when the harvest has finished, finally the combine harvester turns right around to the other long side of partition to continue harvesting until the end of harvest; four sides harvest method is suitable for large fields, after cutting out of road, the combine harvester harvests along the left side of terraces

until the end, then turns right to continue to harvest, and so forth, until the harvest ends. Based on the above practices, the detected straight line is put on the left side of combine harvester.

### 3.1 Image Processing Steps

Images are taken by JAI CV-M77 camera, shooting frame rate of 25s-1, 640×480 color images. Test image was shot in wheat field of suburb in Luoyang City, the weather was sunny. Before the test, the camera is mounted on top of the center-left position combines, apart from the ground about 3m, camera and horizontal's angle about 40°. Camera adopted isolation pads and protected cover with a dust wiper for dust treatment.

**Image processing steps:** (1) Grayscale processing. In such issues, as R(red) channel pixel values change more obviously, here R(red) channel is selected to do grayscale image processing; (2) Image noise reduction. In order to reduce noise interference, we use the level of five-point smoothing filter; (3) Thresholding. Because gray-scale distribution images of agricultural scene are complex, an improved maximum entropy thresholding method for image thresholding is chosen after the test; (4) Morphological processing. To further reduce interference, morphological processing is used with the binary image, processing methods are 3×3 structure element for corrosion and 3×3 structure element expansion; (5) Determination of the candidate point set. Figure 3 shows the average gray value distribution of each line (horizontal) pixels, we can see the gray value become smaller and smaller from top to down. In addition, because the camera is mounted on the top left of center combines harvester, and the straight line angle is generally between  $\pm 10^\circ$ , so the line to be detected appears in the image between the 150 column-the 450 column, the collection point set D method is: scan the nearest point of left side of the 450 column from the 10 row to the 470 row, stop until the 140 column. If there is the point, it should be inserted point set D, if not, go to the next row; (6) At last, use improved HT based on a determined point to complete the line detection. The image processing steps are shown in Fig.2.

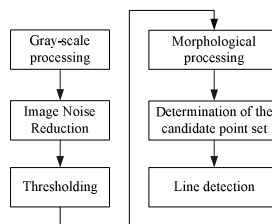


**Fig. 2.** Image processing flow chart

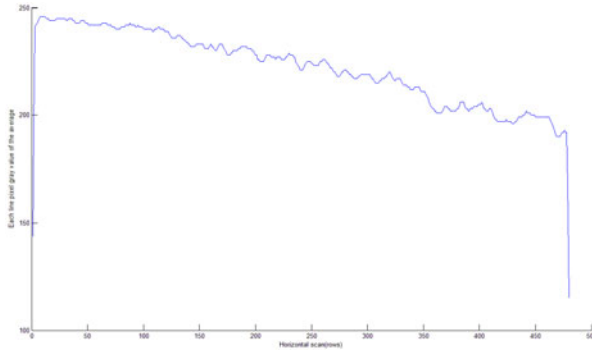


**Fig. 3.** Average gray value distribution of each line (horizontal) pixels

### 3.2 Improved Maximum Entropy Thresholding Method

Because Gray-scale distribution of agricultural scene images is complicated, it is difficult to use a fixed threshold segmentation method, so we choose the adaptive threshold segmentation, currently, adaptive thresholding methods are: Otsu thresholding method [9~10], iterative thresholding method [11] and maximum entropy thresholding method [12]. By using three methods of image segmentation, the segmentation results are shown in Fig.4. It is easy to see from four charts, Fig.4d is the best, so we choose the one-dimensional maximum entropy thresholding method as thresholding method of this study.

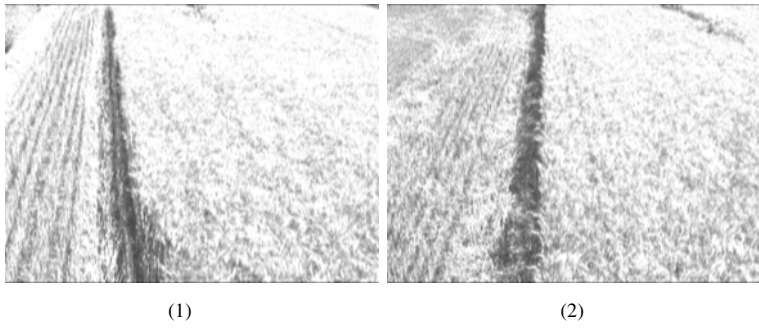
Maximum entropy thresholding method put the concept of Shannon entropy into image thresholding, whose basic idea is that image information entropy is defined by gray-scale image distribution density function and according to different assumptions or different perspectives, there is different entropy criteria, and finally get threshold through optimization of the threshold criteria. Maximum entropy thresholding method has two types: one-dimensional maximum entropy thresholding method and two-dimensional maximum entropy thresholding method.

#### (1) one-dimensional maximum entropy thresholding method

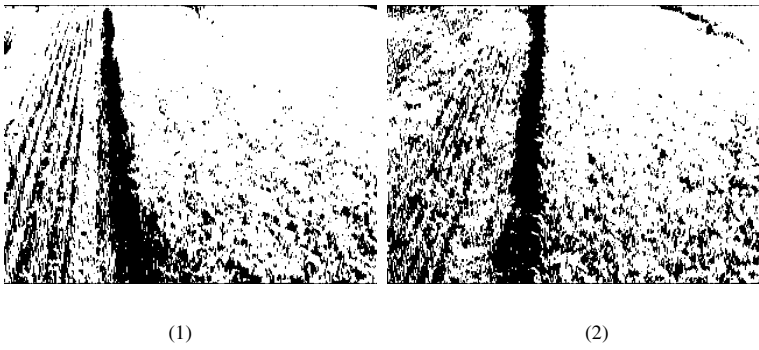
According to information theory, entropy is defined as

$$H = -\int_{-\infty}^{+\infty} p(x) \cdot \lg p(x) dx. \quad (1)$$

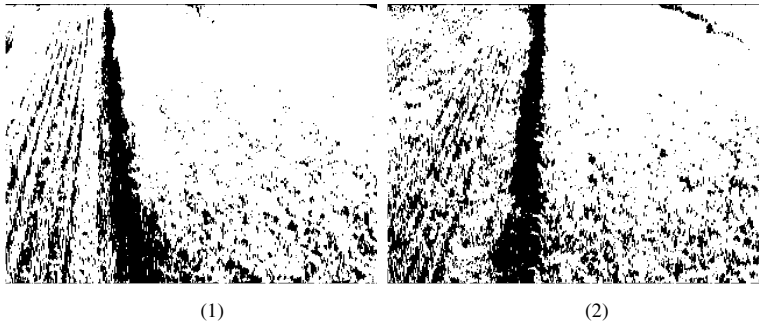
Where  $p(x)$  is the probability density function of random variable  $x$ .



a) Grayscale image



b) Otsu thresholding image



c) Iterative thresholding image

**Fig. 4.** Image segmentation result

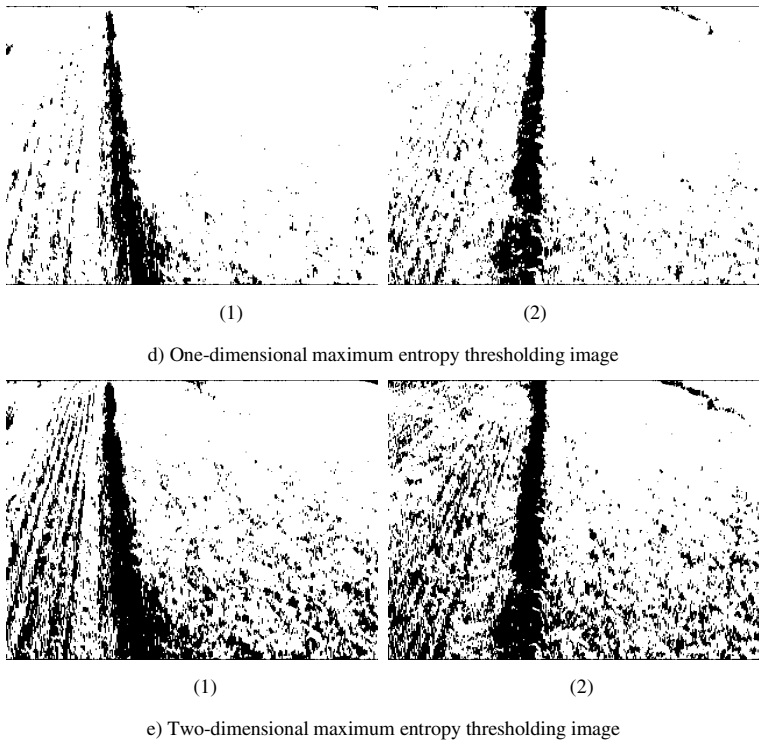


**Fig. 4.** (Continued)

For digital images, random variable  $x$  can be gray value or regional gray, gradient and other characteristics. The words one-dimensional gray-scale maximum entropy mean that the threshold which is chosen can split image into two parts, and the two parts' first-order gray-scale statistics has maximum amount of information. The histogram is shown in Fig.5, we assume that the original grayscale image has  $L$  gray levels, pixel points that are lower than  $t$  gray level constitute the target area  $O$ , and pixel points that are higher than  $t$  gray level constitute the background area  $B$ , so the probability distribution in its region is as follows:

$$\text{area } O : p_i / p_t \quad i = 1, 2, \dots, t ;$$

$$\text{area } B : p_i / (1 - p_t) \quad i = t + 1, t + 2, \dots, L.$$

Thereinto,

$$p_t = \sum_{i=1}^t p_i .$$

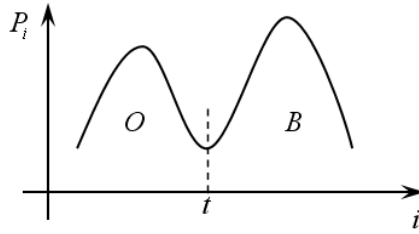


Fig. 5. One-dimensional histogram

For digital images, the target area and background area of entropy are:

$$\begin{cases} H_O(t) = -\sum_i (p_i / p_t) \cdot \lg(p_i / p_t) & i = 1, 2, \dots, t \\ H_B(t) = -\sum_i [p_i / (1 - p_t)] \cdot \lg[p_i / (1 - p_t)] & t = t + 1, t + 2, \dots, L \end{cases} \quad (2)$$

So the entropy function is defined as:

$$\begin{cases} \varphi(t) = H_O + H_B = \lg[p_t \cdot (1 - p_t)] + \frac{H_t}{p_t} + \frac{H_L - H_t}{1 - p_t} \\ H_t = -\sum_i p_i \cdot \lg p_i & i = 1, 2, \dots, t \\ H_L = -\sum_i p_i \cdot \lg p_i & i = i + 1, i + 2, \dots, L \end{cases} \quad (3)$$

When entropy function obtains the maximum, the corresponding gray value  $t^*$  is the desired optimal threshold, the calculation formula is as follows:

$$t^* = \arg \max\{\varphi(t)\}. \quad (4)$$

Because the process of finding  $t^*$  is global search, so the calculation time is too long, so we did some improvement with one-dimensional maximum entropy thresholding method as follows: Since gray level distribution of the medium shot is between the close shot and long shot, we select gray-scale image from the 200 row to the 249 row as a processing unit after numerous tests, then calculate the average gray value  $T$  of this unit, and  $0.75T \leq t^* \leq 1.25T \leq 255$ , thus it greatly reduces the search space of  $t^*$  and saves computing time.

### 3.3 Improved Hough Transform

Linear equations in polar form as:



$$\rho = x \cdot \cos \theta + y \cdot \sin \theta . \quad (5)$$

Where  $(x, y)$  is the Cartesian coordinates of image;  $\theta$  is the angle between the x-axis forward direction and normal line, the range of angle is  $[-90^\circ, 90^\circ]$ ;  $\rho$  is the vertical distance from the line to the coordinates origin. According to geometry, we can see that any two points can determine the line's parameters  $(\rho, \theta)$ .  $a(x', y')$  which is supposed a determined point on a straight line, and  $b(x_i, y_i)$  is a point from candidate set D,  $\rho$  and  $\theta$  can use the formula (6) and formula (7) to calculate:

$$\theta_i = -\tan^{-1} \left( \frac{x_i - x'}{y_i - y'} \right) . \quad (6)$$

$$\rho_i = x' \cos \theta_i + y' \sin \theta_i . \quad (7)$$

The value of  $\theta$  is mapped to a set of accumulators, and each obtained  $\theta_i$  makes the corresponding accumulator value plus 1. Because the points on a same line have the same value of  $\theta$ , so when there is a straight line, its corresponding accumulator has partial maximum,  $\theta_i$  which corresponded partial maximum become  $\theta$  of the request line. According to  $\theta$  and  $a(x', y')$ , the corresponding  $\rho$  value can be got from formula (7).

### 3.4 Walking Goal Line Parameter Calculation

In order to use the Hough transform based on a determined point[13~15], at first, we should confirm this point. As the long shot image has better effect, so we determine the method after many tests as follows: the first 40 points of the set of points  $D(x_i, y_i)$  are taken, then we can determine a point  $a(x', y')$  coordinates value as follows:

$$x' = \bar{x} = \frac{1}{40} \sum_{i=1}^{40} x_i; y' = \bar{y} = \frac{1}{40} \sum_{i=1}^{40} y_i . \quad (8)$$

First, the accumulator A is defined in  $[-15^\circ, 15^\circ]$  range, and the range is divided into 100 equal parts  $A_i$  ( $0 < i < 101$ ), whose amplitude is  $0.3^\circ$ . Then  $a(x', y')$  and the candidate point set  $D(x_i, y_i)$  as the basis, use formula (2) calculation  $\theta_i$ , then map  $\theta_i$  to 100 portions and make the cumulative device  $A_i$  ( $0 < i < 101$ ) value of the corresponding portions plus 1. When mapping has been completed, there must be an accumulator  $A_i$  maximum value, and use the midpoint of this accumulator corresponding parts as the request linear parameter  $\theta$ , according to the formula (3) and  $a(x', y')$ , then calculate the other line A parameter  $\rho$ .

Test results of the image are shown in Figure 6, four images obtained a straight line parameters  $\rho$  and  $\theta$  as follows: Fig.6a is 179.578, -6.45; Fig.6b is 312.155, 7.35; Fig.6c is 269.831, 1.95; Fig.6d is 250.817, -6.75.

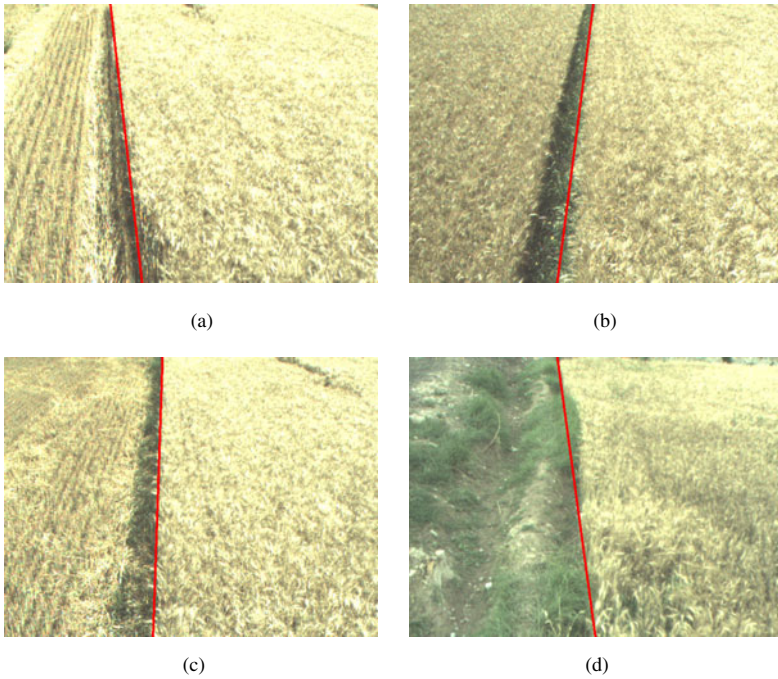


**Fig. 6.** Image results of the experiment

## 4 Conclusion

In allusion to aided driving by harvesting robot, in order to make sure the entire image processing in real time and system can be working long-time stability, so this paper chooses TI's TMS320DM6437 as core processor for the system, meanwhile, the improved Hough transform based on a determined point is applied to complete line detection, the algorithm simplifies binary map to unitary map. Comparing with the traditional Hough transform, it saves computing time, reduces the parameter space greatly, and avoids invalid samples and cumulative problems. In addition, the algorithm is well proved with respect to its anti-interference and robustness etc. Tests show that the entire hardware system is capable of working stably, and the entire system operating time from the acquisition parameters to display is only 40ms or so, obviously, this design can meet the real-time processing requirements. Time is calculated by the time DSP debugging software CCS3.3.

**Acknowledgements.** The authors thank "Twelfth Five-Year" National Technology Key Project (Funding No.: 2011BAD20B00), for their financial support.

## References

1. Zhou, J., Ji, C., Liu, C.: Visual navigation system of agricultural wheeled-mobile robot. *Transactions of the Chinese Society for Agricultural Machinery* 36(3), 90–94 (2005)
2. Shen, M., Ji, C.: Development and Prospect of Vision Guidance of Agricultural Robot. *Transactions of the Chinese Society for Agricultural Machinery* 32(1), 109–110 (2001)
3. Zhao, B., Wang, M., Mao, E., Zhang, X., Song, Z.: Recognition and classification for vision navigation application environment of agricultural vehicle. *Transactions of the Chinese Society for Agricultural Machinery* 40(7), 166–170 (2009)
4. Ma, Z.-F., Zhao, B.-J., He, P.-K.: High-Speed Image Sampling And Detection System Based on DSPC64X. *Transactions of Beijing Institute of Technology* 25(7), 628–631 (2005)
5. Cao, Q., Wang, K., Yang, Y., Shi, X.: Identifying the navigation route based on TMS320DM642 for agriculture visual robot. *Transactions of the Chinese Society for Agricultural Machinery* 40(7), 171–175 (2009)
6. Texas Instruments, TVP5146[S].8(SLES084C) (2007)
7. Texas Instruments, TMS320DM6437 Digital Media Processor[S], 6(SPRS345D) (2008)
8. Ni, C., Li, X., Wang, X.: *Grain harvesting machinery Insider*. Publishing house of electronics industry, Beijing (2008)
9. Navon, E., Miller, O., Averbuch, A.: Color image segmentation based on adaptive local thresholds. *Image and Vision Computing* 23(1), 69–85 (2005)
10. Otsu, N.: A Threshold Selection Method From Gray Level Histograms. *IEEE Trans. on Syst. Man Cybernet SMC-9*, 62–66 (1979)
11. Ridler, T.W., Calvard, S.: Picture thresholding using an iterative selection method. *IEEE Transactions on Systems, Man and Cybernetics*, 630–632 (1978)
12. Guo, H., Tian, T., Wang, L., Zhang, C.: Image Segmentation Using the Maximum Entropy of the Two-Dimensional Bound Histogram. *Acta Optica Sinica* 26(4), 506–509 (2006)
13. Zhang, F., Wang, K., Shi, X.: Vehicle flow detection system based on machine vision. *Control & Automation* 24, 138–140 (2008)
14. Cao, Q., Wang, K.: Vision Navigation Based on Agricultural Non-structural Characteristic. *Transactions of the Chinese Society for Agricultural Machinery* 40(1), 187–189 (2009)
15. Zhao, Y., Chen, B., Wang, S., Dai, F.: Fast detection of furrows based on machine vision on autonomous mobile robot. *Transactions of the Chinese Society for Agricultural Machinery* 37(4), 83–86 (2006)